Probe-Sample Interaction: Lateral Forces

The nature of frictional forces

Lateral forces (besides normal to the surface forces) arise from the tip-surface interaction. AFM allows to measure these forces thereby expanding surface analysis ability for various samples. This technique is called the **Lateral Force Microscopy (LFM)**.
What is the nature of lateral forces and what additional information about a surface they can reveal? There are two forces having horizontal component – frictional force F_t and normal load N which deviates from vertical due to the surface asperities **(Fig. 1)**.
The latter force is entirely determined by the surface relief. Thus, lateral forces give information about the surface topography; however, existence of other developed imaging techniques lowers the experimental value of lateral forces imaging.

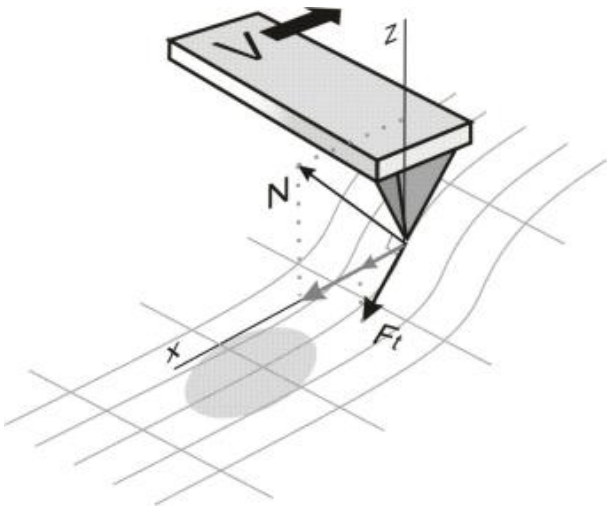

Fig. 1. The nature of lateral forces

On the other hand, friction force study can result in obtaining new data about surface properties. This made the AFM an important tool for **the tribology** – the physical science studying the nature of friction.

Depending on the scale of the friction study, the modern tribology is divided into three fields:
- Macrotribology (or just tribology);
- Microtribology;
- Nanotribology.

Since their emergence, the scanning microscopes offer an ability to study micro/nanotribology. Below we present some essential principles of tribology and discuss the technique of lateral forces investigation.

The frictional force is an aggregate effect arising from various physical phenomena: elasticity, adhesion, viscosity, capillary forces, surface chemistry, phononic and electrostatic interaction, etc. Any of them can dominate depending on conditions.
Each tribology field investigates friction at its own scale. Macrotribology deals with large objects and do not take into consideration a matter structure. On the contrary, nanotribology explains friction on the level of individual atoms interaction. Microtribology is an intermediate field.

Macrotribology
basic law is **the Amontons-Coulomb law** stating that the friction force is proportional to the loading (normal) force:

$$F_{tp} = kN \qquad (1)$$

where k – dimensionless coefficient of friction containing all the tribology information. It depends on many factors, such as temperature, humidity, sliding velocity, etc.

In macrotribology, it is considered that geometrical contact area of two bodies is equal to (or slightly differs from) the real contact area on the atomic scale. This is certainly an approximation because in fact even very flat surfaces seem rough at lower

scale, so the true contact area is much less – only asperities are in perfect contact. At the macroscale, the contact is a great number of microcontacts **(Fig.2)**. In this case, the macroscopic frictional force is an averaged microscopic frictional force of individual microcontacts that can vary greatly.

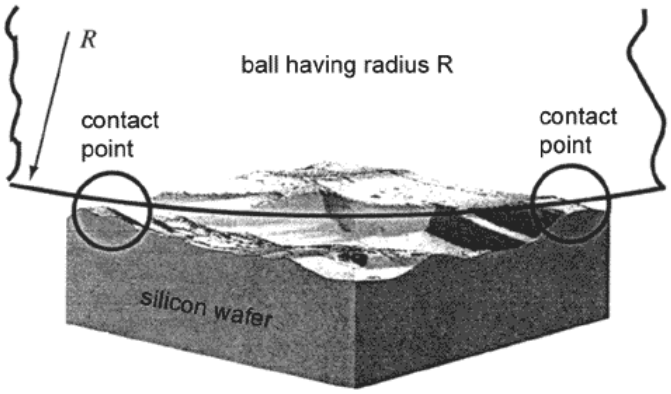

Fig. 2. Ball-silicon wafer contact on the macroscopic scale [1].

Microtribology

studies such individual contacts. As a rule, it is implied that a small single asperity interacts with a surface. Namely this model made the AFM an attractive experimental tool for microtribological studies.

As it is well known, friction is the dissipative force. When the two surfaces in contact slide against each other, mechanical energy dissipation occurs. For example, to maintain constant sliding velocity, an internal force must produce work, therefore, every factor giving rise to friction has a mechanism of the energy dissipation. Considering microtribology, let us list some of them.

Friction can be either dry or wet. It is considered to be wet even when an extremely thin (few atomic layers) film of liquid occurs on the surface. Due to the adsorption this is always the case except for the following:

1. hydrophobic surfaces of tip and sample;
2. friction in vacuum;
3. large normal load resulting in squeezing out of the liquid from the interface, true contact of surfaces establishing and actual realization of the dry friction mechanisma.

It is considered that in case of dry friction surface asperities hit against each other. While overcoming obstacles, atomic-lattice vibrations are generated and dissipated as phonons which carry away the energy. Moreover, when adhesion links between hills of surfaces in contact are broken, electron-hole pairs are created in metallic samples and this process also requires energy (this effect is much weaker than phononic dissipation). In case of soft samples, microasperities can be destroyed (the so called "plowing") and mechanical energy is spent on atomic links break.

Wet friction depends much on liquid layer thickness. If a film is monomolecular, friction is dry-like. If a film is two-three monolayers thick, the energy dissipation in a phonon channel is blocked and liquid layer viscosity is of major importance. For more thick films capillary effects predominate which results in contacting surfaces asperities attraction upon shear.

What is the relation between frictional force and loading force in microtribology? The Amontons-Coulomb low analogue here is **the Bowden-Tabor relation (model)** written as:

$$F_{tp} = \tau A_{\tau} \qquad (2)$$

where τ – shear stress, A_{τ} – true area of elementary contact (in contrast to geometrical contact area in macrotribology). This area depends on degree of both contacting surface hills mutual indenting. As it is known, the area of such contact is given by the Hertz theory:

$$F_{tp} = \tau\pi\left(\frac{RN}{K}\right)^{\frac{2}{3}} \qquad (3)$$

where R – tip radius of curvature, N – normal loading force, K – reduced Young's modulus, given by

$$\frac{1}{K} = \frac{3}{4}\left(\frac{1-\mu'^2}{E'} + \frac{1-\mu^2}{E}\right) \qquad (4)$$

with E, E' – Young's moduli and μ, μ' – Poisson's ratios of tip and sample, respectively. For the silicon probe and sample $E = E' = 150GPa$, $\mu = \mu' \approx 0{,}3$, $K = 110GPa$.

As it can be seen, dependence of the frictional force on normal load N is nonlinear. If a film of liquid exists, it is necessary to add to$N$ an adhesion term

arising from the capillary force. Using the DMT model, it can be written as:

$$F_c = 4\pi\gamma R \qquad (5)$$

where γ – surface tension coefficient. This is the additional attractive force between the contacting surfaces.

The Bowden-Tabor model is verified well in experiments. In **Fig. 3** are shown experimental data [1] acquired in vacuum (lack of liquid film and capillary effect) and in air; theoretical curve (3) is presented for comparison.

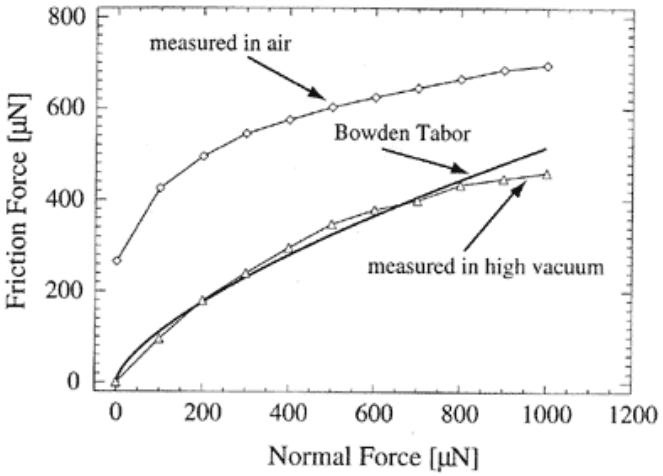

Fig. 3. Experimental frictional force as a function of normal load in air and in vacuum. Thick line shows theoretical Bowden-Tabor relation [1]

In microtribology, the phenomenon such as **"stick-slip" motion** is frequently observed. The frictional force between the two sliding surfaces is irregular and is of saw-tooth character **(Fig. 4)**. If a hill of one surface is stuck to a "site" of the other surface via adhesion and capillary forces, it will hardly be unstuck without predominant force. Once it is separated, it jumps (slips) into another "site" where sticks for a while and so on.

The stick-slip behaviour depends much on scan speed **(Fig. 5)**. To investigate the dependence between frictional force and slip speed, the experiment was carried out [1]. In this experiment the frictional force was measured between silicon ball having radius 0.5 mm and flat silicon surface. Both bodies were hydrophilic. The roughness was 0.2 nm and 0.17 nm for the ball and surface respectively. At low speed the stick-slip phenomenon is pronounced, the jumps frequency is small and amplitude is large. Increasing the speed results in rising the frequency and lowering the amplitude. At some maximum critical sliding velocity the effect vanishes and frictional force becomes regular. In experiment the critical speed 0.4 μm/s was reached at normal load equal 70 μN.

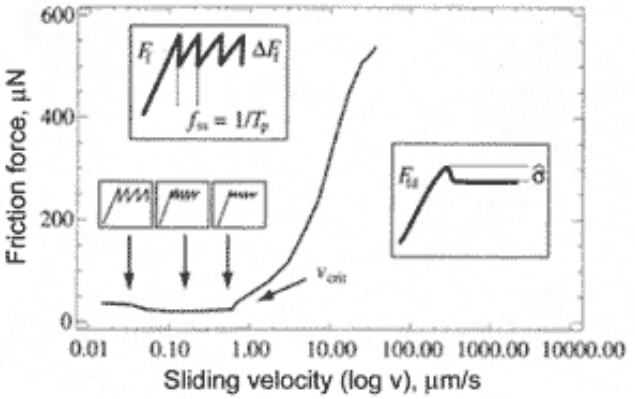

Fig. 4. Frictional force vs. sliding velocity [1]. Frictional force behavior at sliding velocities above and under critical is shown in boxes

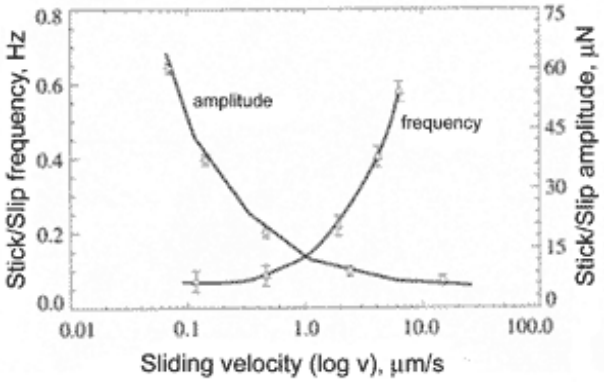

Fig. 5. Frictional force amplitude and frequency at stick-slip motion as a function of scan speed [1]

On the same samples the dependence between frictional force and temperature/humidity was studied[1]. From the beginning both solids were hydrophilic. Then, in order to remove the oxide film and make them hydrophobic, they were etched in hydrofluoric acid for two minutes.

Thus, the frictional force was measured versus relative humidity (RH) at various temperatures for hydrophilic and hydrophobic samples. The measuring system was placed into a camera with adjustable humidity and temperature. RH was in the range from 85% to 20%. The normal load was maintained constant and amounted $N = 2000$ μN. The results for high and low temperatures are shown in **Fig. 6** [1].

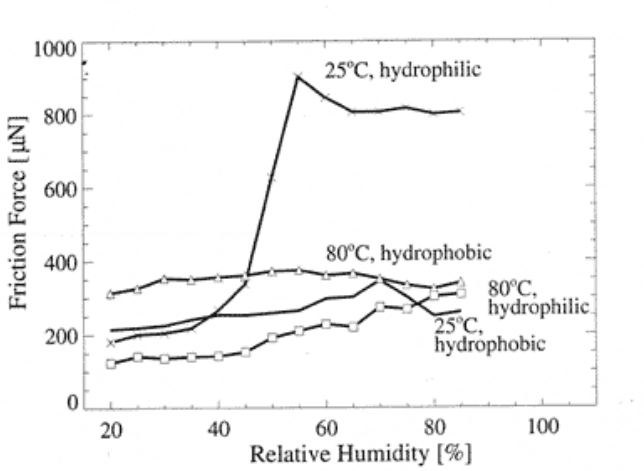

Fig. 6. Friction vs. humidity at various temperatures for hydrophilic and hydrophobic systems [1]

The hydrophilic sample can adsorb ample quantity of water. Thus, the more the environment humidity is, the more liquid can be adsorbed and the higher the frictional force is. As the temperature grows, desorption starts to prevail over adsorption and friction decreases. The more the temperature is, the more energetic water molecules are and the easier they leave the surface and return to it. That is why friction slightly depends on humidity.

Hydrophobic silicon, in contrast to the hydrophilic one, reveals weak dependence of friction on humidity at any temperature. With temperature growth, the friction slightly rises. This means that, as a result of desorption, solid surfaces are in tighter contact, Van der Waals forces start to act between them and chemical bonds arise.

Nanotribology
deals with individual atoms interaction. Imagine a surface atom of one body (AFM tip) that slides in a periodic potential of surface atoms of the other body (sample) **(Fig. 7)** and the energy is not dissipated.

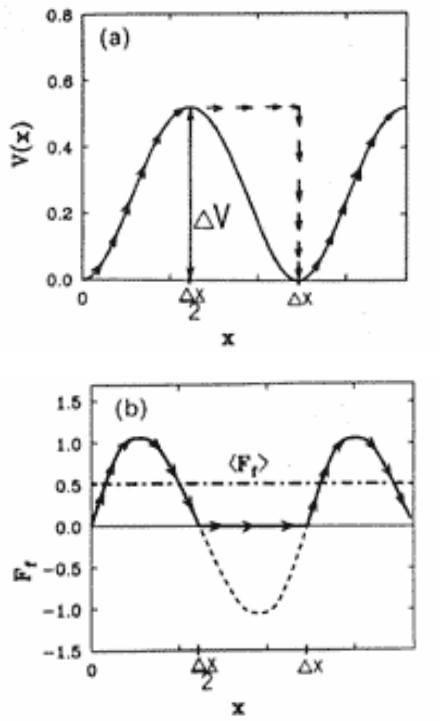

Fig. 7. Left: Potential energy and tip path. Right: Instantaneous and average frictional force [3]

Nonconservatism is introduced as follows. Reaching the point of potential maximum, the atom, which can be modeled as a spring suspended ball, loses contact with the surface and "falls" to the point of potential minimum (or its neighborhood).

The atom passes into the site with another energy, i.e. the potential becomes "nonpotential". The instantaneous frictional force in this case is

$$F_{tp}(\chi) = \frac{\partial V(\chi)}{\partial \chi}, \text{ if } 0 < \chi < \frac{\Delta\chi}{2}$$

$$F_{tp}(\chi) = 0, \text{ if } \frac{\Delta\chi}{2} < \chi < \Delta\chi \qquad (6)$$

It may be thought that thanks to the spring suspension, the energy is transmitted deep into the body, i.e. from the nanoscopic point of view it is dissipated. This model leads to a nonconservative (on average) force shown in Fig. 7 which is the frictional force. This averaged nonconservative

force is considered to be the frictional force in microtribology.

As an example, we present experimental data [2], [4] **(Fig. 8)** obtained for highly oriented pyrolytic graphite (HOPG).

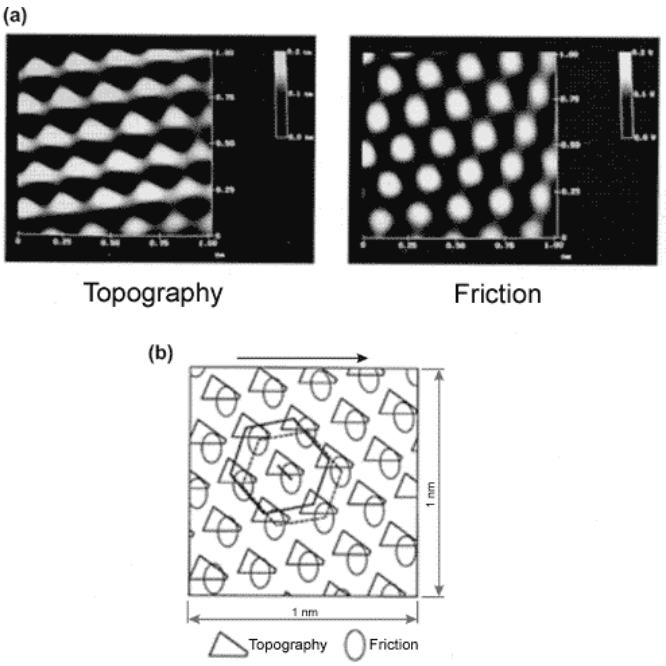

Fig. 8. (a) Topography and frictional force images for the HOPG sample sized 1 nm x 1 nm. (b) Schematic overlay of the two images. Symbols mark corresponding maximums. Spatial shift between images is clearly seen [2], [4]

It is seen that the surface topography and frictional force image are of the same periodicity and shifted relative each other in accordance with the above presented theory.

Notice that the HOPG surface should be dry. Water adsorption in this case is of greater significance than on the microscopic scale. Capillary forces damp stick-slip motion so the acquired image becomes fuzzy

Summary

- The science of friction – tribology – is subdivided into macrotribology, microtribology, and nanotribology. To describe friction at different scales, various models are used.
- The friction depends sufficiently on humidity, temperature, adsorption, etc. and can be of dry or wet type.
- The basic equation of macrotribology is the Amontons-Coulomb law. The macroscopic area of contacting bodies is considered to be multiple elementary contacts whose total area is much less than the gross contact area.
- Dry friction in the elementary contact is described by the Bowden-Tabor model. It employs the Hertzian theory on the elastic deformation in place of contact, the friction parameter being the shear stress.
- Capillary forces are of major importance in the wet friction.
- In microtribology, "stick-slip" phenomenon results in the frictional force irregularity and its saw-toothed variation.
- The nanotribology describes friction in terms of atoms interaction. Considering the motion of one body atoms in the potential of the other body atoms, it is possible to introduce the nonconservative force describing friction.

References

1. Scherge Matthias, Biological micro- and nanotribology: Nature's solutions. Springer, 2001
2. N.P. D'Costa, J.H. Hoh, Rev. Sci.Instrum. 66 (1995) 5096-5097
3. Wiesendanger R., Guentherodt H.-J. (eds.), Scanning tunneling microscopy. - 2d ed. 3 : Theory of STM and related scanning probe methods. 1996
4. Bhushan B., Wear 225-229 (1999) 465-492.

Cantilever deformations under the influence of lateral forces

To investigate friction, the **Lateral Force Microscopy (LFM)** is used. It is based on the probe lateral deflection recording during scanning. In the LFM, the cantilevers in the form of rectangular beam having length l, width w, and thickness t ending with a tip having length l_{tip} **(Fig. 1)**, are used.

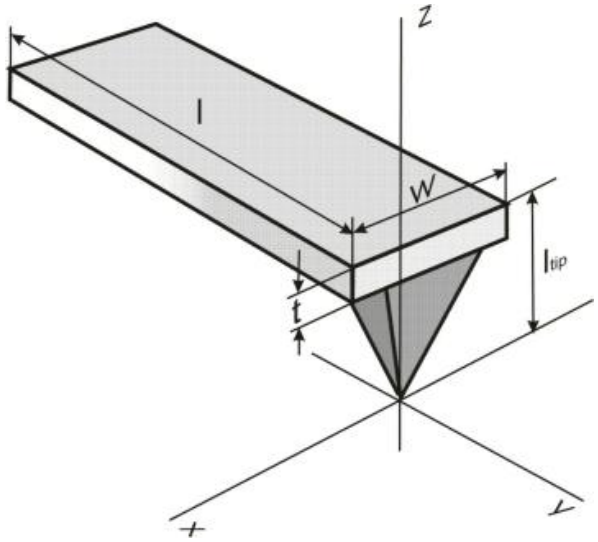

Fig. 1. Rectangular cantilever with tip

When the cantilever moves in the direction $O\chi$ perpendicular to its axis, the tip twists due to the friction. As shown in chapter "Deflections under the transverse force" "Deflections under the transverse force" the twisting angle β is connected with horizontal lateral force F_χ as

$$\beta = \frac{2l_{tip}}{l^2} cF_\chi \qquad (1)$$

where $1/c$ – inverse stiffness coefficient which is defined in (12) chapter 2.1.2 "Deflections under the vertical (normal) force component". The optical system registers this twist as a signal $LAT \sim \beta$.

Another scan mode is available. Scanning in the Oy direction produces frictional force directed longitudinally that results in the vertical beam deformation (see chapter "Deflections under the longitudinal force" "Deflections under the longitudinal force"). In this case the angle of bend α is connected with longitudial force F_y as

$$\alpha = \frac{3l_{tip}}{l^2} cF_y \qquad (2)$$

Emphasize that the bend is due to not only lateral force α but also vertical force component F_z. Therefore, in general case, it is necessary to extend the expression (2) using formulas from chapter "Deflections under the longitudinal force" "Deflections under the longitudinal force":

$$\alpha = \frac{3l_{tip}}{l^2} cFy + \frac{3}{2l} cF_z \qquad (3)$$

In spite of the fact that first component of expression (3) includes a small factor l_{tip}/l, both term can be the same order, because the forces ratio F_y/F_z is sufficiently great and ordinary varies from 1 to 100. The bend with angle α results in a signal $DFL \sim \alpha$.
Thus using optical detection system it is impossible to isolate the value of lateral component F_y. For its determination one should, for instance, find the force F_z by others methods, and then subtract corresponding component from expression (3). Apparently, that this method is more difficult than first, in which the scanning is carried out in a transverse direction and F_χ component can be received immediately.

Summary

- Forces of friction can be measured both at transverse scanning – $\beta = \frac{2l_{tip}}{l^2} cF_\chi$, and at longitudinal – $\alpha = \frac{3l_{tip}}{l^2} cF_y$.
- The transverse scan direction is more preferred, because the cantilever torsion registers as a separate signal LAT.
- At longitudinal scan direction it will be difficult to extract from a signal DFL the value of friction force because essentially of large strains due to normal load influence.
- The influencing of a surface topography on a signal LAT is considered in chapter Qualitative interpretation of results.

References

1. Handbook of Micro/Nanotribology / Ed. by Bhushan Bharat. - 2d ed. - Boca Raton etc.: CRC press, 1999.

Calibration of the optical detection system

Having got a notion about the relation between the lateral forces and cantilever deformations (Chapter "Cantilever deformations under the influence of lateral forces"), let us discuss the calibration of the detection unit. Tilts a and b of the cantilever mirrored side result in the reflected laser beam deflection. The laser spot that strikes a photodetector moves along corresponding perpendicular axes a and b (Fig. 1).

$$\alpha = 2L\alpha\,,\ b = 2L\beta \qquad (2)$$

where L – optical "arm" (distance between mirror and the photodiode). The nonzero beam vertical bending $(\alpha \neq 0)$ leads to the spot travel in the a direction which produces DFL signal while torsion $(\beta \neq 0)$ – to the travel in the b direction and signal *LAT* appearance.

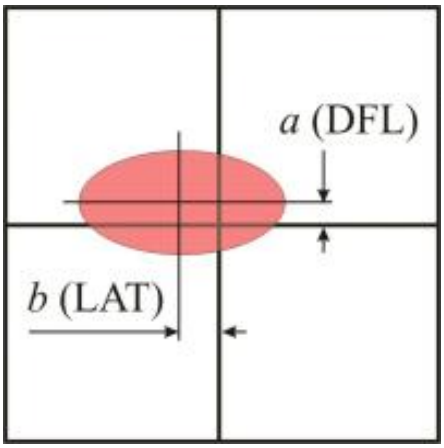

Fig. 1. Spot displacement on the photodetector

Let us introduce constants of proportionality A, B [nA/mm] between a and DFL, b and LAT:

$$DFL = Aa\,,\ LAT = Bb \qquad (3)$$

We have to admit that the spot in the photodetector plane can be noncircular and have irregular shape and even irregular intensity. This originates from the focusing inaccuracy, laser beam diffraction on the cantilever mirrored surface, etc. Nevertheless, at small displacements *a* and *b* (which is true in practice), corresponding signals DFL and LAT are linear in accordance with (3).

Thus, *A* and *B* are the constants of the instrument with the specific cantilever installed. One can determine them by performing the needed calibration procedure that will allow to calculate the spot displacement on the photodiode knowing the signals *DFL* and *LAT*. For that, it is necessary to measure signals amplitude at known displacements *a* and *b*. To produce the known (adjustable) displacements, it is more convenient to move the photodiode rather than deflect the beam (as in case of the cantilever deformation) that is to use the adjustment screws of the photodiode.

Align the beam – it should strike the photodiode reflecting off the non-deflected cantilever. Using the photodiode adjustment screws, move it along perpendicular axes **(Fig. 2)** ξ and η registering signals *DFL* and *LAT* after every turn.

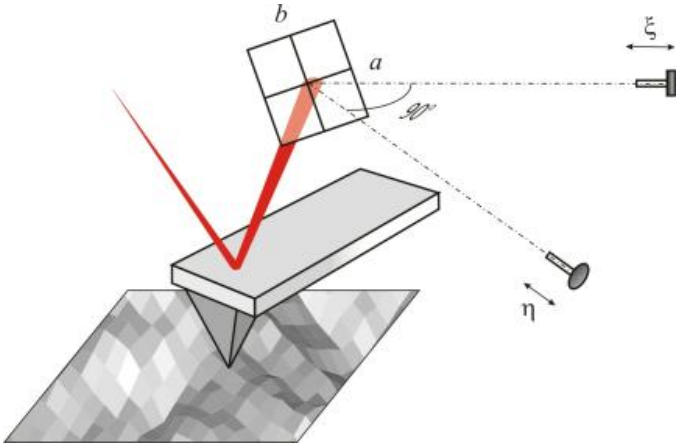

Fig. 2. Optical detection system

Thus plot relations *DFL(ξ)*, *LAT(ξ)* and *DFL(η)*, *LAT(η)*. **Fig. 4** shows the first of them.

Select a interesting region of Fig.3 using mouse pointer

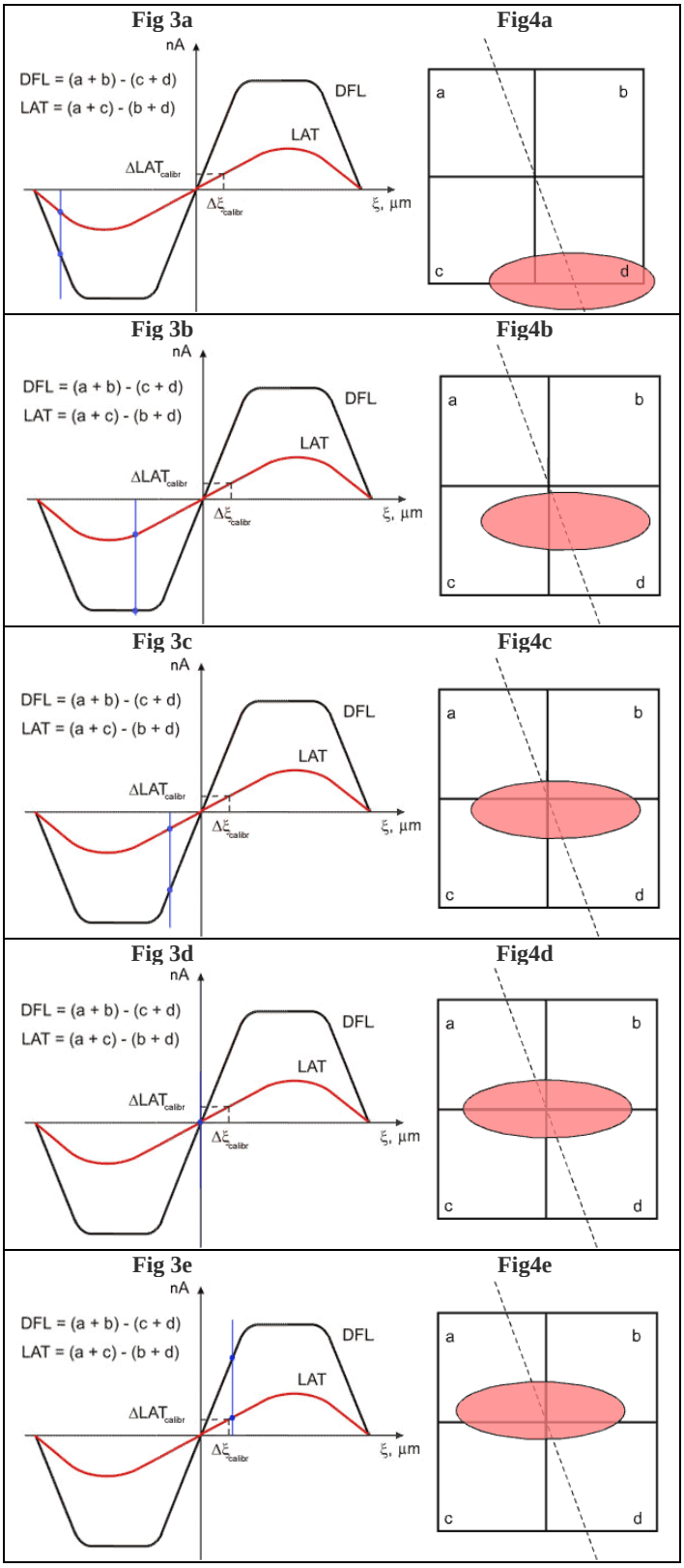

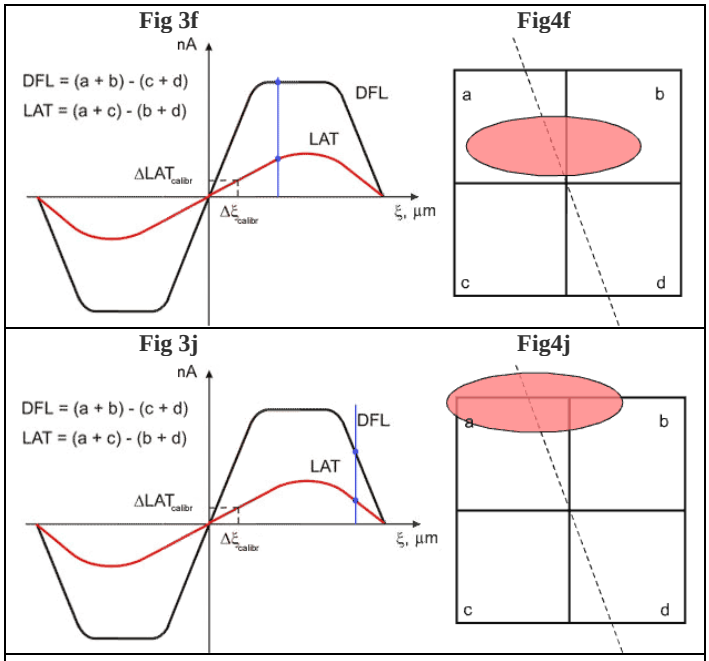

Fig. 3. Ideal relations DFL(x), LAT(x).

Fig. 4. Location of laser beam spot on photodetector corresponding selected ragion of Fig. 4

A linear signals variation near zero point turns gradually into a plateau which correspond to a complete spot shift into one of the photodiode segments. When the spot oversteps the diode limits, signal amplitude starts to decrease. This is an ideal case. In practice, plots look more complicated due to the spot irregularity (see APPENDIX II).

Now, determine what spot displacements in the photodiode co-ordinates (axes *a* and *b*) are produced by screws ξ and η move. Let us find, for example, the change in coordinate a of the spot upon the photodiode move by distance ξ along the same axis. Not taking into consideration the actual axes direction, suppose that in **Fig. 5** the beam strikes the photodiode vertically (beam is always orthogonal the diode) and axis ξ of the diode move is directed arbitrarily. Points *OO'D* form a right triangle.

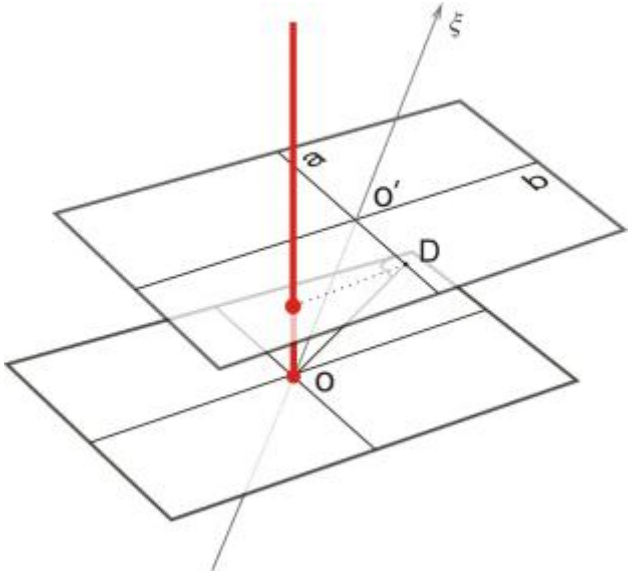

Fig. 5. On expressions (4 - 5)

Then,

$$\alpha = \xi\cos(\xi a),\ b = \xi\cos(\xi, b) \qquad (4)$$

and similarly

$$a = \eta\cos(\eta, a),\ b = \eta\cos(\eta, b) \qquad (5)$$

Angles (ξa), (ξb), (η, a), (η, b) depend on the microscope optical system design and are given in APPENDIX I.

Having got four relations of (4–5) type, it is possible to "rescale" horizontal axes of plots in **Fig. 3.** Slope ratio of plots linear portions are calibration constants *A* and *B*. Generally, to perform signals *LAT* and *DFL* calibration, a couple of plots (one for *DFL*, the other for *LAT*) and two of mentioned angles are enough. However, for some microscope models one or two (of four) plots can degenerate into a horizontal line that makes calibration impossible (see example in APPENDIX II *DFL(η) = 0*).

Finally, to relate the measured signal with a lateral force acting in the x-direction, expressions (1) – (5) are combined to give

$$F_x = \frac{l^2}{4l_{tip}LBc}LAT \qquad (6)$$

where calibration constant B is determined as shown above, for example, from the slope of the LAT(x) plot linear portion (Fig. 3):

$$B = \frac{\Delta LAT_{calibr}}{\Delta\eta_{calibr}\cos(\eta, b)} \qquad (7)$$

Quantitative estimates of the constant *B* and coefficient of arbitrary units used in LFM conversion into force units are presented in APPENDIX II.

Summary

- To measure the lateral force, it is necessary to calibrate the microscope optical detection system that allows for the LAT signal conversion into corresponding force.
- Calibration is performed using the photodiode adjusting screws. For calculations, one should know cantilever characteristics and employ reference data on microscope Solver P47 various models design, given in APPENDIX I.

Qualitative interpretation of results

The relation between detected signal and the lateral force acting in the x-direction is given by:

$$F_x = \frac{cl^2}{4l_{tip}LB}LAT \qquad (1)$$

where calibration constant B is determined in accordance with procedure presented in the chapter Calibration of the optical detection system:

$$B = \frac{\Delta LAT_{calibr}}{\Delta\xi_{calibr}\cos(\xi, b)} \qquad (2)$$

Before interpreting LFM measurements we must learn to differentiate the frictional force effect from the topography effect.

Let us examine the measured lateral forces and their relation with the frictional force. Both in the first (lateral scanning) and in the second (scanning along the beam length) scan modes it is impossible to measure the frictional force in a single pass. The reason is that lateral forces are influenced by both friction and surface topography. As is shown in **Fig. 1**, the normal load has a horizontal component at inclined surface features.

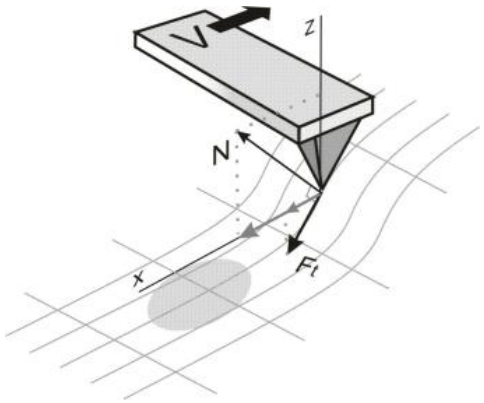

Fig. 1. Detected lateral forces

Therefore, the measured lateral forces contain information about both friction distribution and surface topography. To separate the tribological effect from the topographic effect, it is just enough to reverse the scan direction. The frictional force changes sign in this case while normal load remains the same **(Fig. 2a, 2b)**. The difference of two scan results gives double frictional force while the average result is a sample surface topography **(Fig. 2c)**.

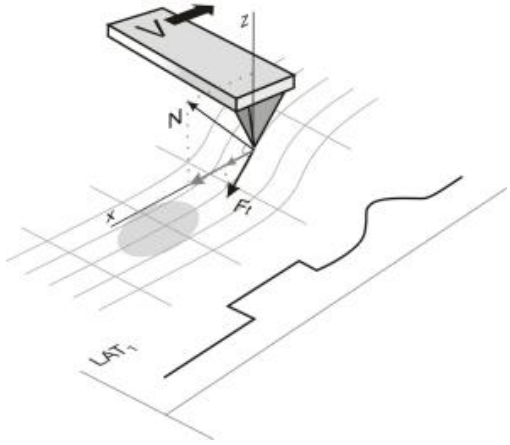

Fig. 2a. Forth scan results

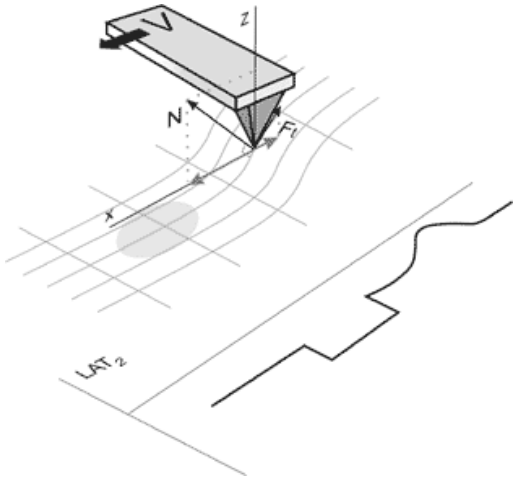

Fig. 2b. Back scan results

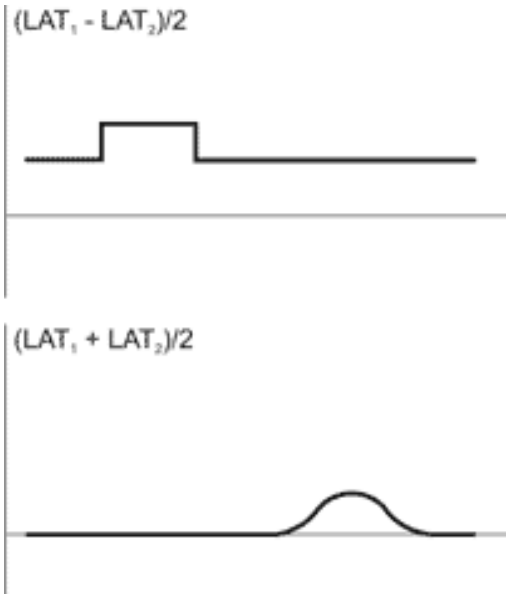

Fig. 2c. Half-difference and average of two scan results

When using the LFM technique, one should remember that during measurements in the contact mode not only the cantilever but also a sample is deformed. It is "indented" which can result in artifacts during both topography imaging and lateral forces mapping.

Effective stiffness of surface features should be much more than the tip stiffness. Only in this case when "indenting" can be neglected, one can obtain true results of lateral forces measurement.

Summary

- Frictional force can be detected along with other lateral forces, the major of which is the normal load horizontal component.
- To separate the frictional force from the total lateral force, it is necessary to reverse the scan direction. Signals difference for trace and retrace gives double frictional force.
- When scanning soft enough samples, image data are distorted due to the surface deformation.

Stick-slip motion on the nanoscale

Introduction

The nanotribology aim is explanation and modeling of friction on the atomic scale. In contrast to microtribology which operates with notions and terminology of the continuum theory, nanotribology utilizes more fundamental concepts based on individual atoms interaction.
The most available tool for experiments in nanotribology is the atomic force microscope. The probe's tip permits to "sense" friction on a tiny contact area of only few atoms.
Our goal is the construction of the model of friction between a tip and a sample on the nanoscale. We have to describe a cantilever motion and find the frictional force the surface exerts on it at scan. The built-in program allows to carry out numerical calculations and change the model parameters at your discretion.

Cantilever modeling

A cantilever (or, rather, its tip) is simulated by a linear two-dimensional damped oscillator that can vibrate only in the horizontal plane *Oxy*. The oscillator is described by six characteristics: m_x, m_y – effective masses for oscillations in corresponding directions, k_x, k_y – stiffness, γ_x, γ_y – damping factors along *x* and *y* axes.

Tip vertical move is not considered in this model so the *z*-components of cantilever characteristics are not used in calculations.

Sample surface modeling

The distribution of Van der Waals potential of the sample lattice surface (interatomic distance a) at height δ over it is of a periodic character. Potential of a single chain can be calculated precisely (see APPENDIX III). Far enough from the surface $(\delta > 0{,}5a)$, this function can be approximated by the sine function with the period of the sample lattice.
Basing on the calculated Van der Waals potential which determines the interaction energy of a separate ("point-like") atom with a sample, one can find the interaction potential of the whole tip with the surface by summation the obtained in the Appendix function over all the tip atoms. This two-dimensional distribution of the potential of the tip positioned over a given surface point describes the sample in our model. This potential also has the periodic structure reflecting the sample lattice. Note, that one should not confuse this distribution for interaction with an extended object with a usual atomic lattice potential which describes the energy of sample atoms interaction with a point-like particle. In our case, this is the potential of interaction with the whole tip.

The function character depends on the tip curvature radius. The more the radius is, the more smooth is the potential distribution. For quite dull tips (of the order of 100 nm) the function periodic structure disappears. In this case our model is not applied and microtribology should be addressed.

As it follows from calculations in the APPENDIX III (where the Van der Waals potential of a single atom depends on its height over the surface δ), the tip potential depends not only on horizontal coordinates but on the vertical coordinate $(U(x,y,z))$, i.e. on the tip height over the surface. Because scanning occurs at constant height δ, the vertical coordinate contribution is taken into account through potential amplitude U_0. Not going into details, the potential distributions for highly oriented pyrolytic graphite (HOPG) and molybdenite MoS_2 will be approximated by following functions [1], [2]:

$$U_{BOПГ}(x,y) = -U_0\left[2\cos\left(\frac{2\pi}{a}x\right)\cos\left(\frac{2\pi}{a\sqrt{3}}y\right)+\cos\left(\frac{4\pi}{a\sqrt{3}}y\right)\right]$$

$$U_{MoS_2} = U_0\cos\left(\frac{2\pi}{a}x\right)\cos\left(\frac{2\pi}{a\sqrt{3}}y\right) \qquad (1)$$

where a – lattice period. For HOPG the lattice period is 2.46 nm, for molybdenite MoS_2 – 3.16 nm.

One-dimensional model

For qualitative understanding of the nanofriction model we shall consider, first, the one-dimensional model of probe oscillations in one direction along the *Ox*-axis. Potential (1) in this case is reduced (by eliminating non-principal constants) to the following

$$U(x) = -U_0 \cos\left(\frac{2\pi}{a}x\right) \qquad (2)$$

where a – lattice period.

Let cantilever of mass m_x attached to an elastic suspension of stiffness k_x move in potential $U(x)$, a carriage being moved with constant velocity v. The model is described by the following equation [1]:

$$m\ddot{x} = k_x(vt - x) - \frac{dU(x)}{dx} - y\dot{x} \qquad (3)$$

The resulted motion character is depicted in Fig. 1 as a plot $x(t)$. When moving "uphill", the probe experiences negative force from the sample and the spring stretches. Upon reaching the "peak", the probe jumps off and starts to oscillate with damping.

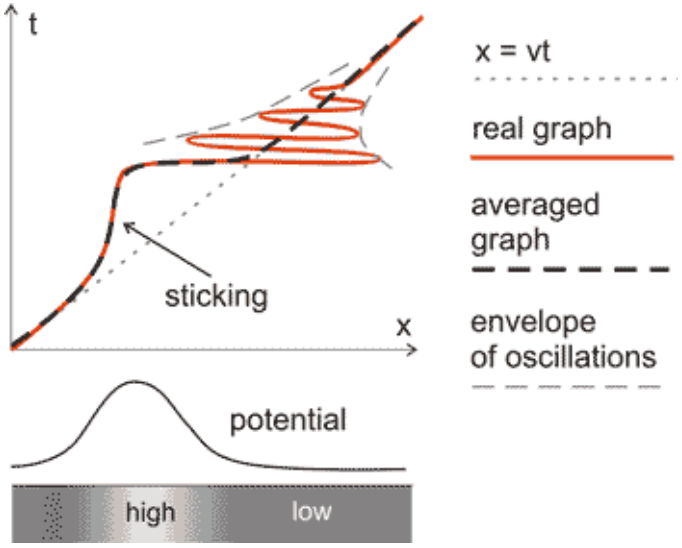

Fig. 1. The probe stick-slip motion in the one-dimensional model

If oscillations are averaged (as shown in Fig. 1 with a dotted line), the jogging motion or the so called "stick-slip" is clearly seen. The frictional force in this case is of the saw-tooth character.

Two-dimensional model

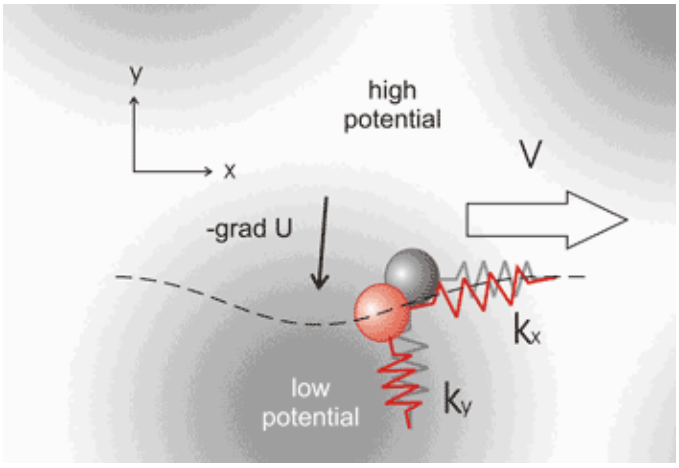

Fig. 2. In the two-dimensional model the probe can deflect laterally. A possible situation in the absence of potential is shown in gray. Actual probe position is shown in red

It is easy to obtain the two-dimensional generalization of the above model (Fig. 2). The following formulas can be written for the case of line $y = Y$ scan in the Ox direction with speed v [3]:

$$m_x\ddot{x} = k_x(vt - x) - \frac{dU(x,y)}{dx} - y_x\dot{x}$$

$$m_y\ddot{y} = k_y(Y - y) - \frac{\delta V(x,y)}{\delta y} - y_y\dot{y} \qquad (4)$$

For the two-dimensional case, the motion has some features. The probe moves not only in the scan direction but from side to side in the *Oy* direction because the tip "slithers" down the potential humps sideways approaching the energy minimum.

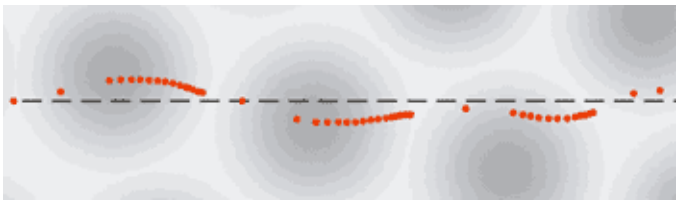

Fig. 3. During scanning the probe moves not only laterally turning round obstacles, but "sticks" ascending the potential maximums. Dotted line shows scan direction, red points correspond to the probe position in equal intervals

In **Fig. 3** dots show a possible trajectory of the tip move. The time interval between dots is the same so one can see that at sites of potential minimum when the probe has to go "uphill" it is delayed while the "downhill" is passed rapidly.

Simplification of calculations

The direct use of formulas (4) in calculations requires large enough computer power. For computation of fast and strongly damped (damping of the order of 10^3) cantilever oscillations it is necessary to use small enough integration time step, so calculations delay.
Within the scope of this model we do not need to reveal details of an oscillation process. It is just enough to trace the tip position averaged over a few periods and not to trace oscillations until total attenuation which is time and resource consuming. If we neglect the second derivative in equations (4), calculations can be noticeably accelerated, the stick-slip behavior being preserved.

$$y_x\dot{x} = k_x(vt - x) - \frac{\delta U(x,y)}{\delta x}$$

$$y_y\dot{y} = k_y(Y - y) - \frac{\delta U(x,y)}{\delta y} \qquad (5)$$

The built-in program features.

In the built-in program (see Flash model) the simplified set of equations (5) without the second derivative (or with zero mass which is the same).

You can choose:

1. model parameters ("Show problem" button)
   - one of two sample materials (highly oriented pyrographite or molybdenite MoS_2)
   - fast scan direction (along or across the cantilever axis)
   - scanning speed (v)
   - cantilever orientation relative to the sample ("scan angle")
   - calculation (not scan!) scheme: only "forth" or "back and forth". (In the second case the running time is double but an image quality at edges is improved due to the lack of an arbitrariness in choosing boundary conditions in every scan line)

2. cantilever parameters:
   - it is possible to choose between one of the standard cantilevers and "My" cantilever typing dimensions of the latter
   - cantilever stiffness (k_x, k_y) along axes being calculated automatically in accordance with formulas (7) in chapter "Deflections under the transverse force" and (10) in chapter "Deflections under the longitudinal force"

3. computation parameters:
   - studied area dimensions
   - number of points along axes

To consider properly the stick-slip motion (and, accordingly, calculate correctly the atomic structure) it is necessary to set more than 30 points of calculation grid per lattice period. This number of points per period is desirable to be integer for obtaining image details. To calculate (and set up) this number, one should know lattice period a, scan size (along fast scan axis) L, points number in line N. Then, number of points per period is $n = \frac{Na}{L}$.
We have to mention how parameters that do not appear in formulas are applied. Setting a sample orientation means the turn of function (2) in plane Oxy by changing of variables using the rotation matrix:

$$\begin{pmatrix} x' \\ y' \end{pmatrix} = \begin{pmatrix} \cos\alpha & -\sin\alpha \\ \sin\alpha & \cos\alpha \end{pmatrix} \begin{pmatrix} x \\ y \end{pmatrix} \qquad (6)$$

where x, y – old coordinates, x', y' – new coordinates, a – rotation angle.

Considering results

The built-in program (see Flash model) allows to depict with shades of grey the deflections of the probe from the non-deformed position along Ox and Oy axes – signals LAT and DFL, respectively. The user can choose any signal distribution to display from the drop-down menu in the top right corner upon calculation completion.
The obtained picture exhibits the periodic behavior corresponding to the lattice period, however maximums of the frictional force are shifted relative to the potential peaks distribution.
From the image one can easily determine the scan direction. Step transitions from light to dark shades correspond to the probe slips after sticking. As the

scan speed increases, the contrast of transitions is lowered.

How to obtain a clear atomic structure image?

How clear is the structure of an atomic lattice being imaged depends sufficiently on the scan direction. **Fig. 4** shows schematically the probe trajectory when scanning along (a) and across (b) atoms chain. As follows from the model, the sticking occurs at lattice points and the probe "slithers" down into these potential minimums (see above "Two-dimensional model").

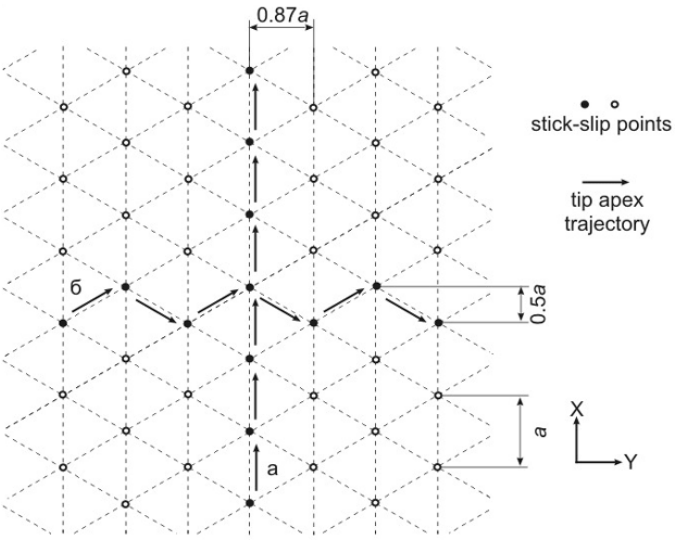

Fig. 4. Probe trajectory during scanning along (a) and across (b) atomic chains.

In case (a) the deflection in the *Oy* direction (across the scan direction) is absent that results in no atomic resolution in the respective signal (LAT or DFL depending on cantilever orientation). Information about the structure will carry only the signal of deflection along *Ox* which will exhibit the saw-tooth profile or stick-slip behavior.

On the other hand, the atomic resolution in line (b) follows from the deflection signal registered in both *Oy* and *Ox* directions. The first of the signals is of the zig-zag form while the second resembles the square-sine function with period $\sqrt{3}a$ because the probe sticks either to the right or to the left from the scan line.

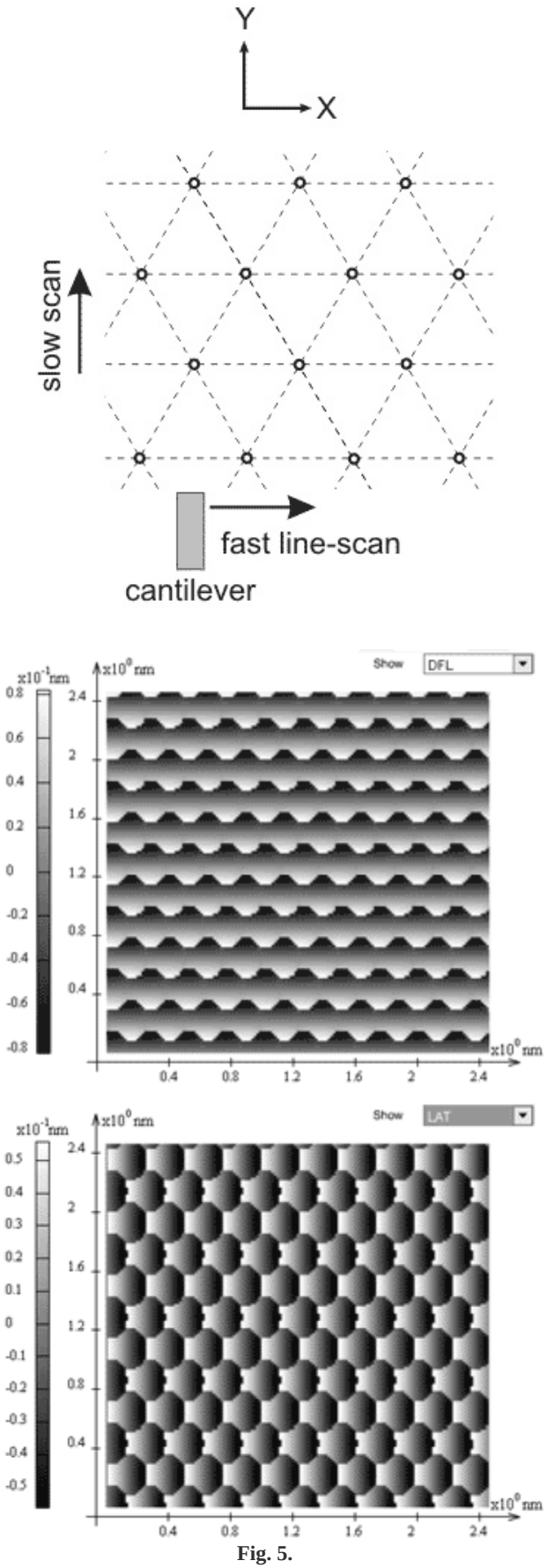

Fig. 5.
(a) – cantilever and fast scan axis orientations relative to the lattice;
(b) – DFL signal distribution;
(c) – LAT signal distribution

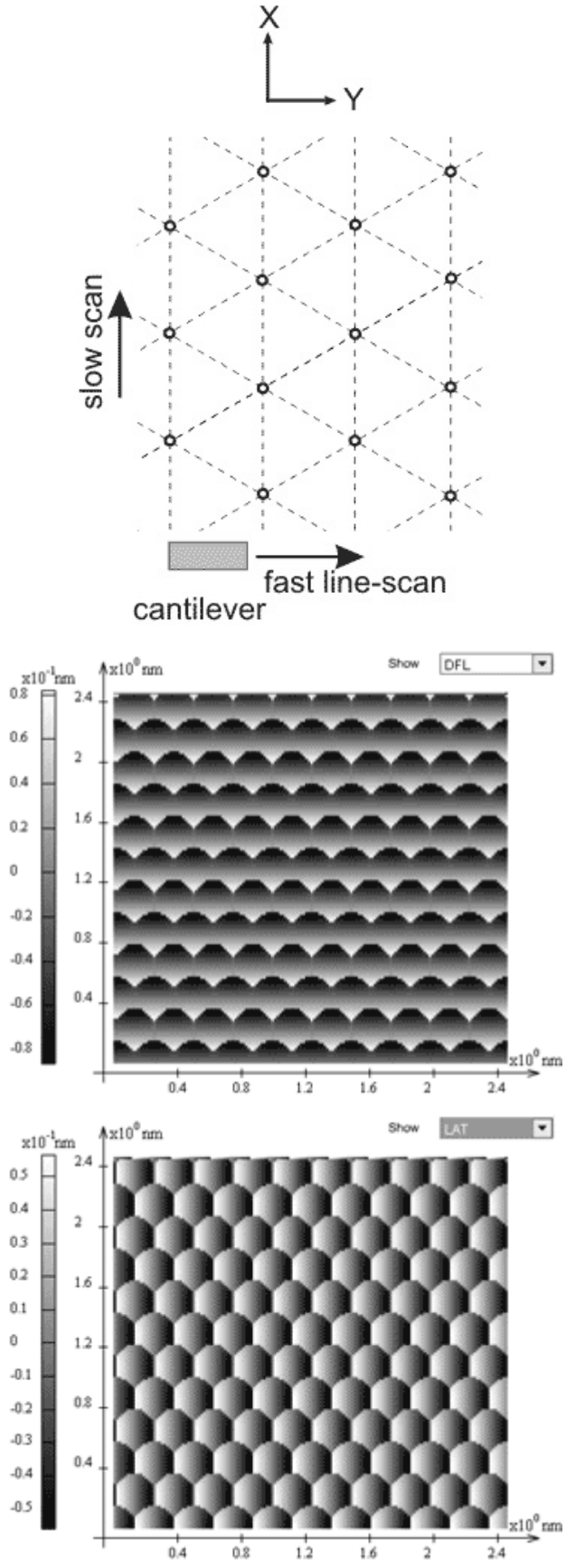

Fig. 6.
(a) – cantilever and fast scan axis orientations relative to the lattice;
(b) – DFL signal distribution;
(c) – LAT signal distribution

References

1. Dedkov G.V., Uspekhi of Physical Sciences, 170 (2000) 585-618 (in Russian).
2. Holscher H., Schwarz U.D., Wiesendanger R., in: Micro/Nanotribology and its Applications, ed. B. Bhushan (Kluwer, Dordrecht, 1997).
3. Holscher H., Physical Review B 57 (1998) 2477-2481.
4. Morita S., Fujisawa S., Sugawara Y., Surf. Sci. Rep. 23 (1996) 1-41.

Stick-slip phenomenon on the microscale

Introduction

In microtribology, the friction is considered on the continuum scale and against nanotribology, the atomic structure of matter is not taken into account. The effective contact area in microtribology is about 100 nm so thousands of atoms participate in molecular interaction. The lattice potential periodic character which plays an important role on the nanoscale, becomes inessential in microtribology because potential features are indistinguishable on this scale.
Our goal is to construct a theoretical friction model on the microscale and creation of the computing algorithm (scheme). In a built-up program based on this one-dimensional numerical model you can change parameters and watch changes in the frictional force during scanning.

We are not going to solve an accurate quantitative problem predicting experimental results but construct a principal model which explains the character of motion, in particular, the so called "stick-slip" motion. Therefore, values of some parameters will be introduced without theoretical substantiation but for the sake of adequacy of obtained results.
As a model object we take a flat sample and a probe in contact with it. The scanning is performed in a contact mode in the direction normal to a cantilever axis.

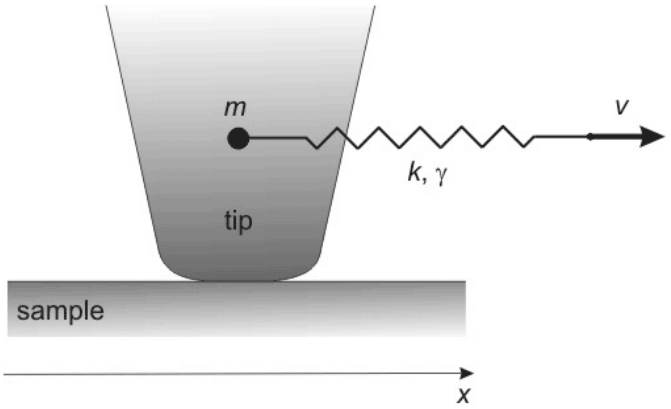

Fig. 1. Cantilever model

Cantilever (or, rather, its tip) is modeled by a linear two-dimensional damped oscillator **(Fig. 1)**. Because we construct the one-dimensional model and scanning is performed in the lateral direction, we shall consider only tip side deflections which are determined mainly by torsion deformation (see chapter "Deflections under the transverse force"). The cantilever is described in this case by three parameters: torsional stiffness k, damping factor in a given direction γ, and oscillator effective mass m.

Cantilever torsional stiffness can be calculated basing on its geometry (see chapter "Deflections under the transverse force"). The mass is determined from the relation

$$m = \frac{k}{\omega^2} \qquad (1)$$

where ω – first mode frequency of torsional oscillations.

For the damping factor we can take the value obtained from the Q-factor of these oscillations Q:

$$\gamma = \frac{\omega}{Q} \qquad (2)$$

Physical fundamentals of the model

While moving along the sample surface, the cantilever experiences an adhesive attraction. In this model, the origin of this interaction is not discussed and its character is just postulated. The nature of adhesion can be different – from interdiffusion of long organic molecules to capillary effect of adsorbed films. The force of adhesion can vary from some minimal value F_b to maximal $F_b + \Delta F$ Introduced is the relaxation time τ during which the attraction force on the immovable tip after contact increases from F_b to $F_b + \Delta F$ [1]:

$$F_{fr} = F_b + \Delta F\left(1 - \exp\left(-t/\tau\right)\right) \qquad (3)$$

In other words, the longer the cantilever is located at a given site, the more it is "stuck". Due to postulating of such kind of friction, arises a non-trivial stick-slip phenomenon that will be discussed later.

Let us introduce such a notion as **"contact age"** φ – effective time of the tip being in contact at given point. The contact age (by definition) is given by integral:

$$\varphi(t) = \int_0^t dt' \exp\left(-\frac{x(t) - x(t')}{D}\right) \qquad (4)$$

In this formula $x(t)$ – function describing the position (coordinate) of the tip during scanning at preceding moments of time. Integration is performed from the contact onset to the current moment. Effective radius of interaction D is the distance which the clamped cantilever end must move to break the contact between the tip and the surface. Although the contact age depends on all the previous scan history, due to the exponent presence only those moments of time when the tip is in the D -vicinity of the given point contribute sufficiently into the integral. Thus, when the cantilever is far from the studied vicinity, the time is "forgotten".

Naturally, for a motionless tip, the contact age is equal to the time that passed from the moment of the contact onset. If the tip moves across the sample uniformly with velocity v, the contact age is the same in all sites and equal to

$$\varphi = \frac{D}{v} \qquad (5)$$

Equations of the model

The tip move obeys the second Newton law [1][5]:

$$m\ddot{x} + my\dot{x} + k(x - vt) = F_{ft} \qquad (6)$$

where F_{fr} depends on contact age (4) as follows:

$$F_{fr} = F_b + \Delta F(1 - \exp(-\varphi/\tau)) \qquad (7)$$

The left hand side includes the cantilever natural elastic force, arising from the probe deflection from the non-deformed position $x_0 = vt$ during scanning, and the damping. The external force represented by the equation right hand side is the microscopic frictional force considered above.

Set of equations (6) and (7) describe the constructed model completely. For the numerical system construction it is convenient to replace integral equation (4) with equivalent differential one:

$$\dot{\varphi} = 1 - \frac{|\dot{x}|\varphi}{D} \qquad (8)$$

To solve system (6-7) numerically, it is brought to the system of three differential equations, then the explicit scheme is utilized.

Stick-slip phenomenon

In the constructed model, a **sticking-sliding phenomenon**, which reflects the saw-tooth behavior of the frictional force in time, can become apparent at certain parameters. For the equations set (6-7) there is the solution instability with respect to small perturbations. The characteristic profile of the frictional force during the unstable motion is depicted in **Fig. 2** [1]–[5]. This is the stick-slip motion: the probe is held at certain sites, the frictional force starts to raise until the probe separation occurs and the frictional force jumps to a certain minimum.

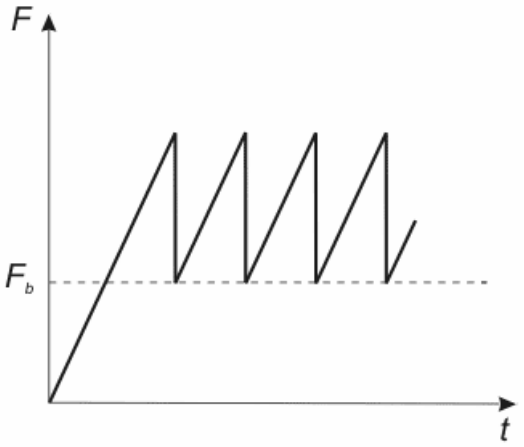

Fig. 2. Plot of frictional force vs. time

The spectral analysis of the linear stability of the model nonlinear equations set allows to determine the critical relationship between problem parameters at which the motion character changes from stable to irregular stick-slip:

$$\frac{k_s}{m} = \left(1 + \frac{v_c}{\gamma D}\right)\left(\frac{\Delta F_0}{m\tau v_c}\exp\left(-\frac{D}{v_c\tau}\right) - \frac{\gamma v_c}{D}\right) \qquad (9)$$

It is important that the character of motion – stable or unstable – depends on scan speed. There exists a certain critical speed v_c below which the uniform sliding transforms into stick-slip. The red curve $v_c(k)$ in the parameters plane (k, v) at the other parameters being fixed, demarcates the regions of stable and unstable motion.

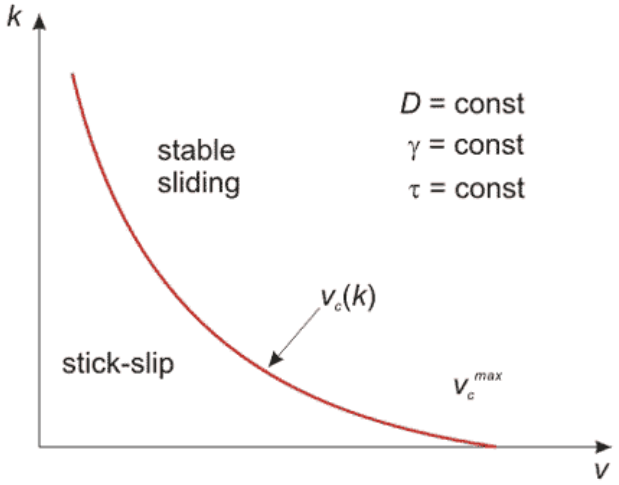

Fig. 3. Regions of stable and stick-slip motion

The plot permits to draw a conclusion that for any stiffness k there is a certain speed v_c over which no stick-slip occurs. Note that there is the maximum speed $v_c^{\max}$ at which (if extremely "soft" cantilever is chosen: $k \to 0$) the stick-slip motion is available.

Expression (4) contains, however, the other model parameters. It is important to discuss how they affect the instability onset. Upon variation of relaxation time τ, interaction radius D, and force change ΔF, the critical curve $v_c(k)$ in **Fig. 3** will shift. One can show that if the following inequality is satisfied

$$\frac{myDe^2}{4\tau\Delta F} > 1 \qquad (10)$$

the region of unstable motion in the plot disappears. This means that at any scan speed the sliding is uniform. Therefore, to reach the stick-slip motion, it is not enough to adjust the speed but it is necessary that relaxation time τ and force variation ΔF are large enough while γ and D are small.

Features of the model numerical realization

Examining equation (2) one can easily reveal its limitation. Once in contact with a sample, an immovable probe should start moving due to the frictional force and that is a physical nonsense. Such errors will arise at rest or at very low probe speed. That is why the model includes a kind of "stabilizer", i.e. the frictional force direction is chosen basing on the following criteria:

$$F_{fr} = \begin{cases} F_b + \Delta F\left(1 - e^{-\varphi/\tau}\right), & if \quad v > 10^{-6} \cdot \dfrac{\Delta F}{k}\omega \\ -\left(F_b + \Delta F\left(1 - e^{-\varphi/\tau}\right)\right), & if \quad v < -10^{-6} \cdot \dfrac{\Delta F}{k}\omega \\ F_b + \Delta F\left(1 - e^{-\varphi/\tau}\right), & if \quad \begin{cases} |v| > 10^{-6} \cdot \dfrac{\Delta F}{k}\omega \\ vt - x > F_b + \Delta F\left(1 - e^{-\varphi/\tau}\right) \end{cases} \\ -\left(F_b + \Delta F\left(1 - e^{-\varphi/\tau}\right)\right), & if \quad \begin{cases} |v| > 10^{-6} \cdot \dfrac{\Delta F}{k}\omega \\ -(vt - x) > F_b + \Delta F\left(1 - e^{-\varphi/\tau}\right) \end{cases} \\ 0, & otherwise \end{cases}$$

(11)

Another feature is that the solution has regions of both gradual and sudden change, the last needed small integration step for the correct calculation. To optimize calculations, the algorithm with an adaptive step was implemented. In case of sudden solution change, the step of difference equations integration is halved, otherwise, it is increased.

Choosing the problem parameters

The cantilever parameters calculation was given above. The other parameters F_b, ΔF, D, τ are chosen empirically so that modeling results are close to experimental. Our goal is not the precise solution of the problem to predict experimental results, but the construction of the principal model explaining stick-slip behavior.
For the majority of materials, the effective sticking (adhesion) radius D should be taken as ~ 0.2 nm and the relaxation time τ as ~ 150 ms. In its turn, the minimum force F_b and force variation ΔF are set taking into account the real friction coefficient of materials and stick-slip appearance.

In the built-in program (see Flash model), the most typical values of listed parameters are set by default which allow to reveal all the microfriction model features:

velocity	v = 5 μm/s
scan region	L = 500 nm
frequency of first torsional mode (for **CSC12(B)** cantilever type)	f_1 = 351.71 kHz
effective mass	m = 6.72 * 10^{-12} kg
Q-factor	Q = 10
damping	γ = 4.91 * 10^5 1/s
minimal force	F_b = 5 * 10^{-7} N
variation of frictional force	ΔF = 10 * 10^{-7} N
relaxation time	τ = 5 ms
interaction radius	D = 0.2 nm.

Let us compare the results of numerical modeling and experimantal data. List of parameters for numerical modeling (**Fig. 4**):

scan velocity	v = 110 μm/s
scan region	L = 11 μm
CSC12(B) cantilever type	
minimal force	F_b = 20 μN
variation of frictional force	ΔF = 50 μN
relaxation time	τ = 5 ms
interaction radius	D = 0.2 nm.

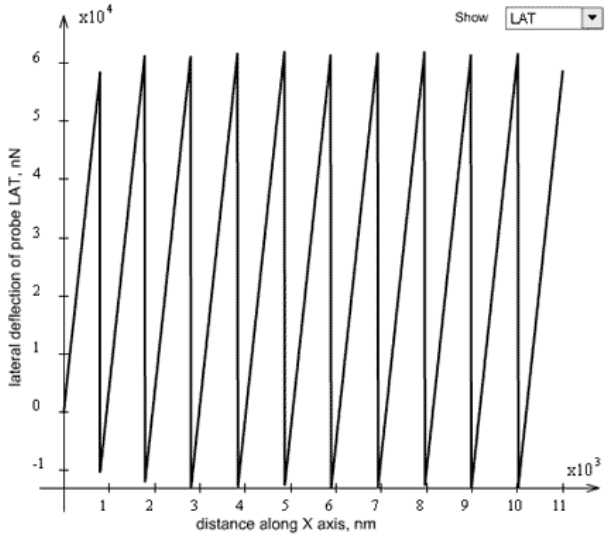

Fig. 4. Results of numerical modeling

List of experimantal parameters (Fig. 5):

scan velocity	v = 110 μm/s
scan region	L = 11 μm
cantilever type	**CSC12(B)**
sample	smooth silicon plate
SetPoint = 0.36 nA (squeeze force 2.1 nN)	

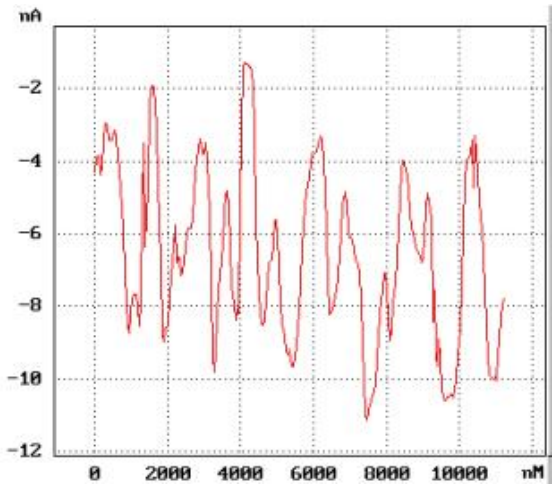

Fig. 5a. Experimantal results. Scan direction: from left to right

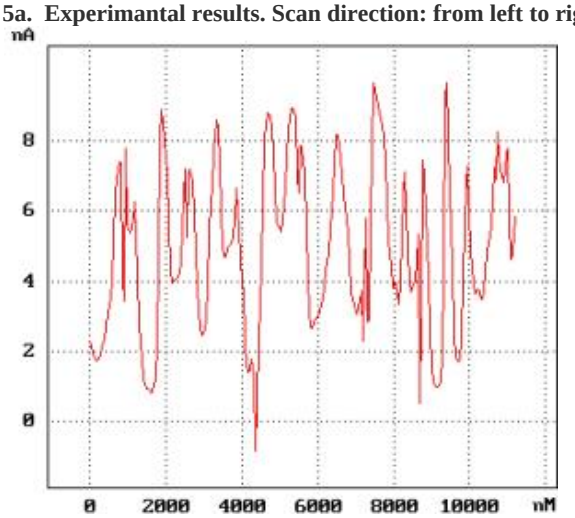

Fig. 5b. Experimantal results. Scan direction: from right to left

Friction force can be calculated by means of the formula (1) in chapter Qualitative interpretation of results: F_b = 170 nN, ΔF = 500 nN.

In accordance with **Fig. 5**, if the scan direction changes the signal **LAT** changes sign on contrary. It means that cantilever twists in different side at opposite scan direction.
A stick-peak period of numerical modeling is in close agreement with experimantal results and approximately equals to ~ 1 μm. However, it should be emphasized that friction force in the numerical model exceeds the experimental condition more than one hundred times.

The built-in program features

The built-in calculation program allows to set up parameters and obtain the evolution in time of the **LAT** signal, which is proportional to the friction force, and to see also the contact age at any time. The user can choose any relation to display from the drop-down menu in the top right corner upon calculation completion.

You can change the following model default parameters:

- Cantilever parameters. It is possible to choose between one of the standard cantilevers and "My" cantilever typing dimensions of the latter, its torsional stiffness k, frequency of first torsional mode and effective mass m being calculated automatically.
- Damping γ
- Minimum frictional force F_b
- Variation of frictional forc ΔF
- Relaxation time τ
- Interaction radius D
- Scan velocity v
- Scan length L

Considering results

Let us examine a few examples. We shall use the default parameters and change only scan speed and relaxation time.

Case 1.
Parameters: τ = 5 ms; v = 5 μm/s; L = 500 nm.

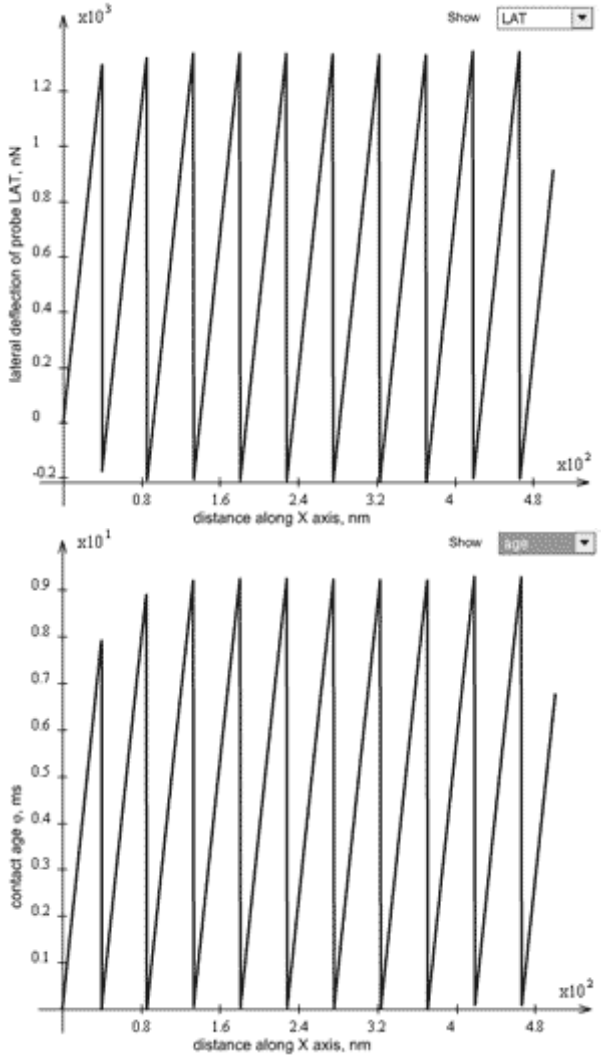

This is a typical stick-slip motion. Parameters point (k,v) is in the unstable area of the plot in **Fig. 3**.

The force (or, rather, **LAT** signal describing the elastic probe deflection under the influence of the friction) is of the saw-tooth form. The contact age changes non-uniformly, too which is the evidence that the probe jogs staying at sites of sticking.

Case 2.
Parameters: τ = 5 μs; v = 5 μm/s; L = 100 nm.

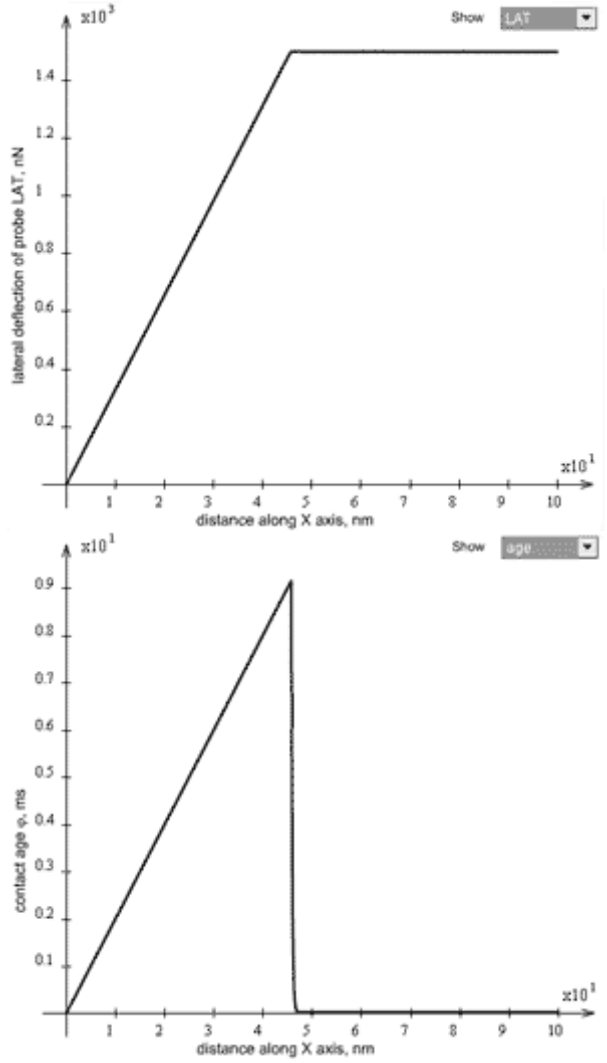

Once started, the probe moves uniformly without stick-slip. At such a small relaxation time τ condition (10) of the lack of unstable region in the plot in **Fig. 3** is satisfied. This in fact means that during the uniform probe move, the relaxation can occur because the contact age (D/v = 40 μs) exceeds much the value of τ. The cantilever in this case experiences the maximum frictional force $F_b + \Delta F$. Examining the contact age plot, one can see that after a delay at the starting point when cantilever was passing into the undeformed state, the contact age becomes constant and equal to D/v.

Case 3.
Parameters: τ = 20 ms; v = 5 μm/s; L = 100 nm.

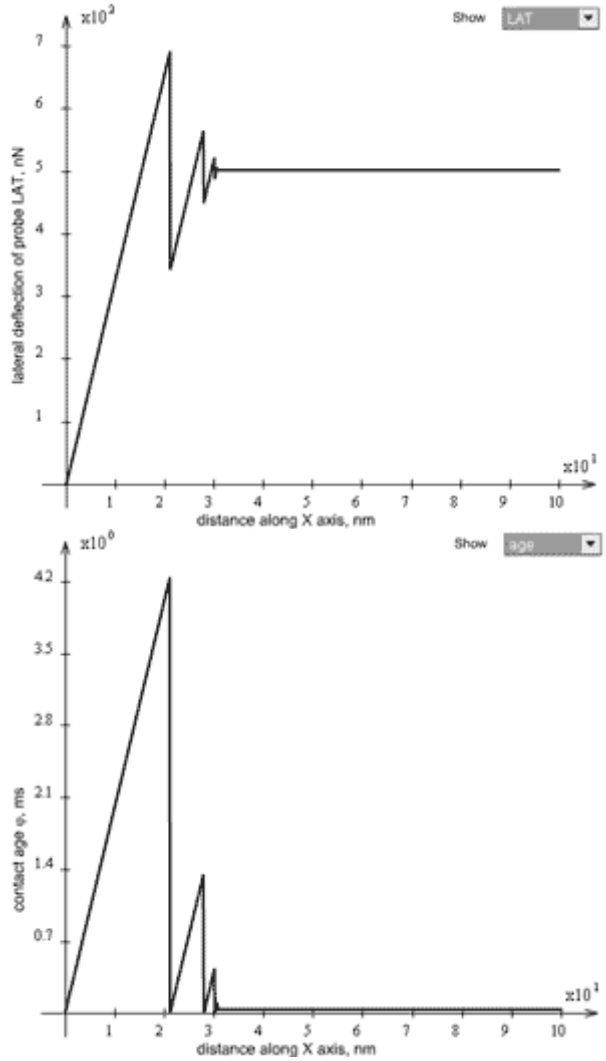

Upon completion of transient processes when probe was joggled to "unstick" from the starting point where it was strongly "stuck", the probe moves uniformly. Due to a large τ value the critical curve in **Fig. 3** moves down and parameters point (k, v) gets into the region of stability. By lowering speed, for example, to v = 1 μm/s, stick-slip motion can be observed again. Instead of speed lowering, the longer cantilever, e.g. **CSC12(D)** having smaller stiffness, can be chosen. In this case, we get into the parameters region where unstable motion takes place.

Case 4.
Parameters: τ = 20 ms; τ = 25 μm/s; L = 100 nm.

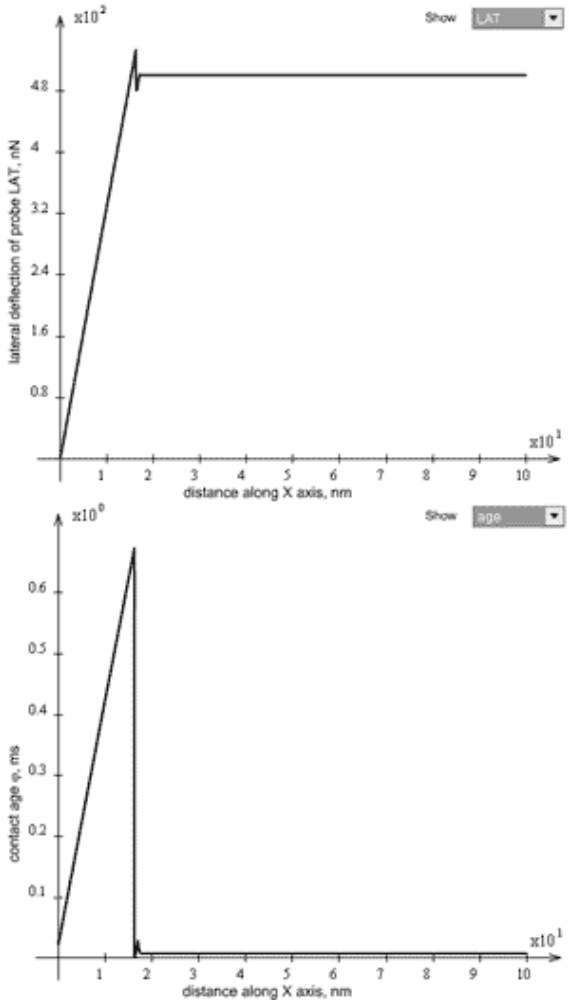

The scan speed is so high that the contact age is only D/v = 8 μs, therefore no relaxation that needs 20000 μs is available. Frictional force equals its minimal value F_b.

Regferences

1. Persson B.N.J., in: Micro/Nanotribology and its Applications, ed. B. Bhushan (Kluwer, Dordrecht, 1997).
2. Meurk A., Tribology Letters 8 (2000) 161-169.
3. Scherge Matthias. Biological micro-and nanotribology: Nature's solutions / Scherge Matthias, Gorb Stanislav N. - Berlin etc.: Springer, 2001. - XIII, 304.
4. Handbook of micro/nanotribology/ Ed. by Bhushan Bharat . - 2d ed. - Boca Raton etc.: CRC press, 1999. - 859.
5. Batista A.A., Carlson J.M., Physical Review E 57 (1998) 4986-4996.

Appendices

APPENDIX I

In the early model of the microscope Solver P47 the cantilever axis is inclined 20° to the sample plane **(Fig. 1)**. The plane of incident and reflected beams is perpendicular to the cantilever axis. The angle between these beams is 40°. The beam reflected off the non-deflected cantilever is perpendicular to the photodiode plane.

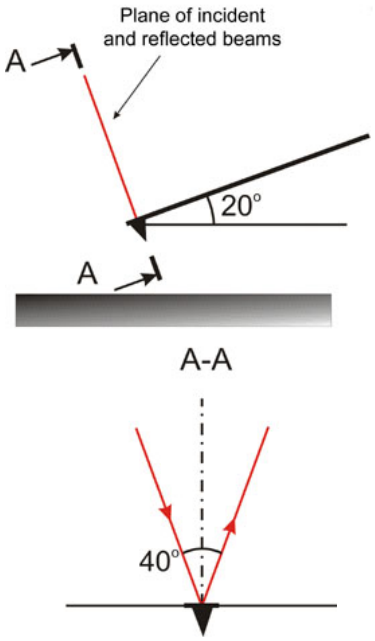

Fig. 1. Optical detection system orientation in space

Omitting calculations, we present the angles value:

	angle, °	cos
(ξa)	20	0.94
(ξb)	83.3	0.12
(η, a)	90	0
(η, a)	20	0.94

APPENDIX II

Given below is an example of the calibration constant calculation (LAT signal vs. lateral force) for the early model of the Solver P47 microscope having silicon cantilever **CSC12** with the following characteristics:

length	l = 90 μm
tip height	l_{tip} = 10 μm
spring constant	$1/c$ = 0.52 N/m

Experimental plots of the DFL and LAT signals vs. adjusting screws travel x and h are shown in Fig. 2

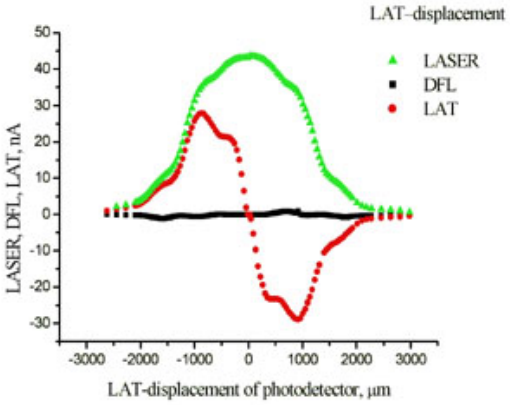

Fig. 2a. Experimental plots DFL(x), LAT(x)

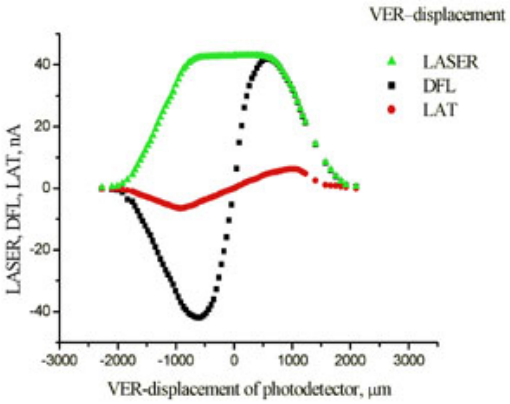

Fig. 2b. Experimental plots DFL(h), LAT(h)

The laser spot on the photodetector is of irregular shape and has irregular intensity. As a result, obtained relations differ from the ideal ones (see Fig. 5 chapter Calibration of the optical detection system). The uneven curve in Fig. 2b is the evidence of the spot intensity side maximums arising apparently from the light diffraction. The reason for the lack of plateau on plots is the spot diameter exceeding half the photodetector size. To determine the B constant, the linear portion of the plot LAT(ξ) in Fig. 2a and data from APPENDIX I are used.

$$B = \frac{\Delta LAT}{\Delta \eta \cos(\eta, b)} = 6.2 \cdot 10^4 \; nA/m$$

Substituting values into expression (2) chapter 2. 6.4, we get

$$F_x[nN] = \frac{l^2}{4 l_{tip} LBc} LAT[nN] = 4{,}2 \cdot LAT[nA]$$

APPENDIX III

Problem

Determine the interaction potential of a polyatomic tip with a surface within the model of the pairwise Van der Waals interaction of individual molecules.

Solution

The potential of two atoms interaction (neutral atoms having no dipole moment) at large (relative to the atom size) separation is given by

$$U(r) = -\frac{C}{r^6} \qquad (1)$$

where r – separation between atoms, C – constant of Van der Waals interaction which can be expressed through atoms polarizability.

Consider potential U_{line} of interaction between an atomic chain of identical atoms separated by distance a and a single atom at distance l from the chain; x is the distance to the neighbor atom along the chain.

It is obvious that

$$U_{line}(l,x) = -\sum_{k=-\infty}^{\infty} \frac{C}{\left(\sqrt{l^2 + (ka+x)^2}\right)^6} \qquad (2)$$

where k – atom number in chain.

Normalizing lengths by period a and introducing designations $\alpha = l/a$ and $\beta = x/a$, we get

$$U_{line}(l,x) = -\frac{C}{a^6}\sum_{k=-\infty}^{\infty} \frac{1}{\left(\alpha^2 + (k+\beta)^2\right)^3} \qquad (3)$$

The sum in this expression can be calculated accurately which gives

$$\sum_{k=-\infty}^{\infty} \frac{1}{\left(\alpha^2 + (k+\beta)^2\right)^3} = -\frac{\pi}{8\alpha^5} \frac{1 + ctg(\pi\beta)^2}{\left(ctg(\pi\beta)^2 + cth(\pi\alpha)^2\right)^3}\left(A\pi^2\alpha^2 + B\pi\alpha + C\right) \qquad (4)$$

where

$$A = 2cth(\pi\alpha)\left(cth(\pi\alpha)^2 - 1\right)\times \left(cth(\pi\alpha)^2 + 3cth(\pi\alpha)^2 ctg(\pi\beta)^2 - 3ctg(\pi\beta)^2 - ctg(\pi\beta)^4\right)$$

$$B = 3\left(cth(\pi\alpha)^2 - 1\right)\left(cth(\pi\alpha)^4 - ctg(\pi\beta)^4\right)$$

$$C = -3cth(\pi\alpha)\left(cth(\pi\alpha)^2 + ctg(\pi\beta)^2\right) \qquad (5)$$

The sum calculation results for two different values of parameter α are shown in **Fig. 1**

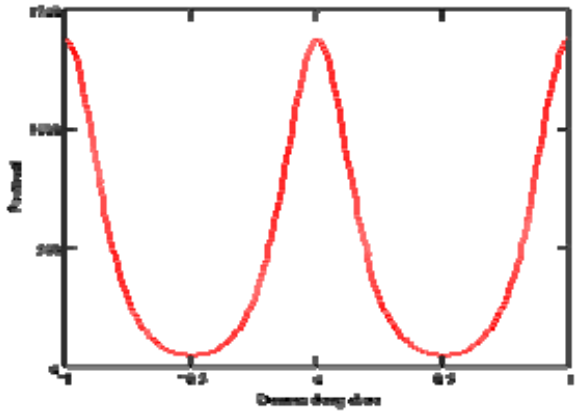

a)

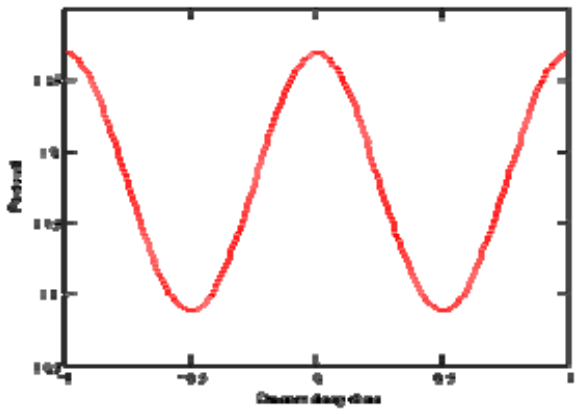

b)

Fig. 1. Dependence of potential (value of dimensionless sum) on atom shiftalong the chain (absciss of both plots is dimensionless parameter β) at constant distance between atom and chain axis: (a) α = 0.3, (b) α = 1

As seen from **Fig. 1a**, at small distance to the chain axis, the potential is of complicated form, but as the distance increases **(Fig. 1b)**, the potential becomes sineshaped. Note that assuming the interatomic potential to be that for the Van der Waals interaction, we thereby supposed that the distance between atoms is more then atom size.

In extreme case of large values $\alpha > 0{,}4$ the sum can be approximated by following expression

$$\sum_{k=-\infty}^{\infty} \frac{1}{\left(\alpha^2 + (k+\beta)^2\right)^3} \approx u_0(\alpha) + u_A(\alpha)\cos(2\pi\beta) \quad (6)$$

where

$$u_0(\alpha) = \frac{3\pi}{8\alpha^5},$$

$$u_A(\alpha) = \frac{\pi\left(4\pi^2\alpha^2 + 6\pi\alpha + 3\right)}{4\alpha^5}\exp(-2\pi\alpha)$$

To obtain the potential of interaction with atomic plane one should sum the derived formula over all atomic chains on the surface properly changing parameter α. However, calculation of such a sum in analytic form is impossible. Nevertheless, the mean value of potential can be easily obtained by reducing summation to integration and assuming that atomic density is "uniformly spread" over a sample volume.

The oscillating term $u_A(\alpha)$ in the formula is responsible for the pseudoatomic resolution of scanning microscopy. Evidently, due to the exponential factor, the noticeable contribution into the interaction can give only neighbor atomic chains. As an example, consider [100] plane of a cubic lattice. The accurate calculation of the contribution of underlying layers into the potential for such a surface do not exceed 0.1%, therefore we shall restrict ourselves to considering only the top layer. Let δ be the dimensionless distance over the surface in α units and γ – dimensionless distance across the chain axis. Then, the potential of interaction with the surface is written as:

$$u(\beta,\gamma,\delta) \approx const + u_B(\gamma,\delta)\cos(2\pi\beta) \quad (7)$$

Taking into account three neighbor atomic chains, we get:

$$u_B(\gamma,\delta) = u_A\left(\sqrt{(1-\gamma)^2+\delta^2}\right) + u_A\left(\sqrt{\gamma^2+\delta^2}\right) + u_A\left(\sqrt{(1+\gamma)^2+\delta^2}\right) \quad (8)$$

Considering only case of large $\delta(\delta > 0{,}5)$ we can obtain a good approximation:

$$u(\beta,\gamma,\delta) \approx const + u_C(\delta)\cos(2\pi\gamma)\cos(2\pi\beta) \quad (9)$$

where

$$u_C(\delta) = 0{,}5u_A(\delta) + u_A\left(\sqrt{\delta^2-1}\right) - u_A\left(\sqrt{\delta^2+0{,}25}\right)$$

Returning to dimensional units, we can write:

$$U_{surf}(x,y,z) = const(z) - \frac{C}{a^6}U_C(z)\cos\left(\frac{2\pi x}{a}\right)\cos\left(\frac{2\pi y}{a}\right) \quad (10)$$

где

$$U_C(z) = \frac{1}{2}u_A\left(\frac{z}{a}\right) + u_A\left(\sqrt{\frac{z^2}{a^2}+1}\right) - u_A\left(\sqrt{\frac{z^2}{a^2}+\frac{1}{4}}\right)$$

Result

The oscillating part of the atom-surface interaction potential at the distance of the order of atomic period and more is the periodic function (cosine) with the period of atomic lattice (for the [100] plane of cubic lattice).

Note

For the other lattice types, e.g. graphite, the contribution of underlying layers can be considerable, therefore, the period in the image can be less than the interatomic distance in the top layer.

CONTACT DETAILS

Building 167, Zelenograd, 124460, Moscow, Russia
Tel: +7(095)535-0305, 913-5736
Fax: +7(095) 535-6410, 913-5739

e-mail: spm@ntmdt.ru; http://www.ntmdt.ru